

# Inverse Gas Chromatography for Determining the Dispersive Surface Free Energy and Acid–Base Interactions of Sheet Molding Compound-Part II 14 Ligno-Cellulosic Fiber Types for Possible Composite Reinforcement

Ryan H. Mills,<sup>1</sup> Douglas J. Gardner,<sup>1</sup> Rupert Wimmer<sup>2</sup>

<sup>1</sup>School of Forest Resources, Advanced Engineered Wood Composites Center, University of Maine, Orono, Maine 04469

<sup>2</sup>University of Natural Resources and Applied Life Sciences, Institute of Wood Science and Technology, BOKU-Vienna, Vienna, Austria

Received 15 April 2008; accepted 9 June 2008

DOI 10.1002/app.28956

Published online 19 September 2008 in Wiley InterScience (www.interscience.wiley.com).

**ABSTRACT:** Composites reinforced with natural plant fibers are currently actively researched. Inverse gas chromatography (IGC) is a technique that is used to characterize the surface energy and polar characteristics of materials. The theoretical approaches used with IGC are reviewed and applied to the study of 14 ligno-cellulosic fiber types including grass fibers, bast fibers, leaf fibers, seed fibers, and fruit fibers. This was done to provide insight into the impact of fiber composition on the surface characteristics of the different fiber types and explore possible correlations among the data. The dispersive surface energy, and  $K_a$ ,  $K_b$

constants are reported for the 14 fiber types and compared with values reported in the literature. The dispersive energies ranged from 35.5 mJ/m<sup>2</sup> to 44.2 mJ/m<sup>2</sup> at 20°C with  $K_a$  from 0.01 to 0.38 and  $K_b$  from 0 to 1.05. A correlation was found at 40°C for surface energy related to fiber composition and fiber type where the surface energy decreases with increasing lignin and hemicellulose composition but increased with increasing cellulose concentration. © 2008 Wiley Periodicals, Inc. *J Appl Polym Sci* 110: 3880–3888, 2008

**Key words:** biofibers; compatibility; surface energy

## INTRODUCTION

### Background

Biobased composite materials are receiving considerable attention for competing with composites derived from petroleum sources. The reinforcement of composites by natural fibers rather than commonly used glass fibers is a field of active research.<sup>1–6</sup> Much attention has been devoted to the study of acid–base characteristics of various pulped products<sup>7–11</sup>; however, relatively little work has been done to characterize other nonwood fiber types. To understand better how a matrix material interacts with a reinforcement fiber, the surface characteristics of both the fiber and matrix material need to be determined. A relatively easy technique for determining surface characteristics of ligno-cellulosic fibers is the technique of inverse gas chromatography (IGC). Therefore, in this article the research questions asked are as follows: (1) To which extent are surface characteristics significantly different among fiber types or at least fiber categories and (2)

is there any coherence between the measured surface characteristics and the chemical composition of the fibers as reported in the literature.

### IGC analysis

Multiple ways to analyze IGC data have been developed in the last few decades.<sup>12–16</sup> Because a number of different fiber types are being analyzed in this article, a short review of the theoretical aspects of IGC analysis follows.

$$V_N = \frac{273.15}{T_c} \times \frac{1}{w} \times Q(t_r - t_i) \quad (1)$$

The retention time measured by IGC is the net retention volume (the volume of carrier gas required to elute a zone of solute vapor) per gram of adsorbent and is determined by eq. (1). Where  $T_c$  is the column temperature,  $w$  is the mass in grams of adsorbent packed into the column,  $Q$  is the corrected flow rate of the helium gas,  $t_r$  and  $t_i$  are the retention time of probe and inert gas. Dorris and Gray<sup>12</sup> introduced the concept of using IGC data to determine the Gibbs free energy ( $G_D$ ) of a solid.

$$\Delta G_D = R \times T \times \ln(V_N) + C \quad (2)$$

Correspondence to: R. H. Mills (ryan.mills@umit.maine.edu).

and,

$$\Delta G_D = N \times a \times W_A \quad (3)$$

Coupling eqs. (2) and (3) with the observation that only dispersive interactions are significant for nonpolar interactions,<sup>13</sup> the work of adhesion ( $W_A$ ) can be written as a geometric mean of the surface energy.

$$W_A = 2 \times (\gamma_S^D \times \gamma_L^D)^{1/2} \quad (4)$$

By combining eqs. (2)–(4), an expression relating the eluted volume to the free surface energy is derived.

$$RT \ln(V_N) = 2 \times N \times (\gamma_S^D)^{1/2} \times a \times (\gamma_L^D)^{1/2} + C \quad (5)$$

Dorris and Gray<sup>12</sup> proposed equations for calculating the London dispersive component of the surface free energy

$$\Delta G_D^{\text{CH}_2} = \frac{RT}{1000} \ln \frac{V_{N(C_{n+1}H_{2n+4})}}{V_{N(C_nH_{n+2})}} \quad (6)$$

and,

$$\gamma_S^D = \frac{1}{4\gamma_{(\text{CH}_2)}} \left[ \frac{\Delta G_D^{\text{CH}_2}}{N \times a_{\text{CH}_2}} \right]^2 \times 10^{12} \quad (7)$$

Where  $\Delta G_D^{\text{CH}_2}$  is the free energy of adsorption for a methylene group,  $R$  is the gas constant,  $n$  is the number of carbon atoms in the alkane probe molecules,  $\gamma_{(\text{CH}_2)}$  is the surface free energy of the methylene group, 35.6 mJ/m<sup>2</sup>,  $N$  is Avogadro's number,  $a$  is the area of an adsorbed methylene group, 6 Å<sup>2</sup>,<sup>13</sup> and the factors 1000 and 10<sup>12</sup> are conversion factors.

Schultz and Lavielle<sup>14,15</sup> graphed  $RT \ln V_N$  versus  $a(\gamma_L^D)^{1/2}$  and found a linear relationship where the slope is  $2N(\gamma_S^D)^{1/2}$  and the intercept is the constant  $C$  in eq. (5) when using alkane, (nonpolar), probes. Polar probes were not found to lie on the linear line created by the alkanes and the perpendicular distance from the alkane line to the polar probe is  $\Delta G^{\text{AB}}$  or  $\Delta G^{\text{SP}}$ .

Donnet et al.<sup>16</sup> developed an analysis where the specific interactions on solid surfaces are determined based on the polarizability of the gas probes. The analysis started with the assumption that two nonidentical molecules that exchange only nondispersive forces can be described by the London equation.<sup>16</sup> The London equation relates the potential energy of interaction,  $\theta_L$ , to the molecules deformation polarizability,  $\alpha_{0,i}$ , characteristic electronic frequency,  $\nu_i$ , distance of the adsorbate to the adsorbent molecules,  $r_{1,2}$ , permittivity in a vacuum,  $\epsilon_0$ , and Planck's constant,  $h$ . The deformation polarizability for the molecules was calculated from the refractive index of the molecules using Debye's equation. After assuming

that the harmonic mean of the molecules electronic frequency can be substituted with the geometric mean, (according to Donnet et al. this introduces less than a 4% error), eq. (8) can be derived.<sup>16</sup>

$$\theta_L = K(h\nu_s)^{1/2} \alpha_{O,S} (h\nu_L)^{1/2} \alpha_{O,L} \quad (8)$$

For the case of the alkane probes where  $\Delta G^{\text{SP}}$  is zero, eq. (8) may be written as:

$$RT \ln V_n + C = \theta_L = K(h\nu_s)^{1/2} \alpha_{O,S} (h\nu_L)^{1/2} \alpha_{O,L} \quad (9)$$

when polar probes are used for testing the surface characteristics,  $\Delta G^{\text{SP}}$  is not zero and is added to eq. (9).

$$\begin{aligned} [-\Delta G_A] &= RT \ln V_n + C = \theta_L \\ &= K(h\nu_s)^{1/2} \alpha_{O,S} (h\nu_L)^{1/2} \alpha_{O,L} + [-\Delta G_A^{\text{SP}}] \end{aligned} \quad (10)$$

As was the case with the Schultz method, the perpendicular distance from the alkane line to the polar probe is the  $\Delta G_A^{\text{SP}}$ . The polarization method was developed because of temperature, partial pressure limitations, and material limitations of the previous methods described.<sup>16</sup>

By running experiments at different temperatures, the free energy of adsorption is measured. The Gibbs free energy of adsorption is related to the enthalpy of adsorption by the following expression:

$$\Delta G^{\text{AB}} = \Delta H^{\text{AB}} - T \Delta S^{\text{AB}} \quad (11)$$

From this equation the enthalpy of adsorption can be determined by plotting  $\Delta G_{\text{AB}}$  versus  $T$  producing a straight line where the intercept is  $\Delta H_{\text{AB}}$ .

Gutmann's approach<sup>17</sup> of using electron donors and acceptors for the enthalpy of acid–base interactions can now be applied.

$$-\Delta H_A^{\text{AB}} = K_A \text{DN} + K_B \text{AN} \quad (12)$$

The DN and AN are the acceptor and donor numbers related to chemical references. The donor number, DN, was defined as the negative of the enthalpy of formation for the chemical made by the acid–base reaction with antimony pentachloride. The corresponding electrophilicity of a chemical species was determined from the <sup>31</sup>P NMR shifts induced by triethylphosphine oxide, a basic probe. The  $K_A$  and the  $K_B$  are constants that show how the solid differs from the references used with the standards.<sup>17</sup>

## MATERIALS AND METHODS

### Sample preparation

Ligno-cellulosic fibers can be divided into several groups depending on the location of the fibers in the

TABLE I  
Physical Constants for Probes Used in IGC Experiments<sup>54</sup>

Probe	Polarizability index		DN (kcal/Mole)	AN* (kcal/Mole)	Specific characteristic
	$\alpha_0(h\nu)^{0.5} \times 10^{49} \text{ C}^{3/2} \text{ m}^2 \text{ V}^{-1/2}$				
<i>n</i> -Octane	11.4		–	–	Nonpolar
<i>n</i> -Nonane	12.5		–	–	Nonpolar
<i>n</i> -Decane*	13.6		–	–	Nonpolar
<i>n</i> -Undecane*	14.7		–	–	Nonpolar
Acetone	5.8		17	2.5	Amphoteric
Chloroform	7.8		–	4.8	Acidic
Tetrahydrofuran	6.8		20	0.5	Basic
Ethyl acetate	7.9		17.1	1.5	Amphoteric

\* Indicates the values were calculated by extrapolation as Donnet et al. did for *n*-Nonane in their original work.<sup>16</sup>

plant, i.e., grass fibers, bast fibers, leaf fibers, and fruit fibers.<sup>18</sup> For grass fibers, wheat straw (*Triticum sp.*), bleached wheat pulp fibers, rice hulls (*Oryza sativa*), and reed (*Phragmites communis*) were selected. For bast fibers, hemp (*Cannabis sativa*), flax (*Linum usitatissimum*), jute (*Corchorus olitorius*), and kenaf (*Hibiscus cannabinus*) were selected. Sisal (*Agave sisalana*) and the banana fiber abaca (*Musa textiles*) represented the leaf-fiber group. Finally, fruit fibers were obtained from unicellular seed or fruit hairs including cotton (*Gossypium*) and poplar hairs as seed hair fibers (*Populus sp.*), and finally kapok (*Ceiba pentandra*) and coir (*Cocos nucifera*) as fruit hair fibers. Most of the fiber types were obtained commercially and the fiber samples were of high quality. With the exception of wheat pulp, the fibers underwent regular processing steps,

such as retting, decortication, separation, cleaning, and drying, with no additional modification treatment done to the fibers. The bleached wheat pulp was directly obtained from a wheat pulp mill and the poplar seed fibers were delivered by a small company that produces special blankets and other bedding products. All fiber types were analyzed by IGC and the results compared with fiber chemistry data obtained from the literature.

The 14 fiber types were sheared in a Wiley Mill until passing through a 0.5 mm diameter screen. The chopped fibers were collected and screened using a 45 mesh screen then followed by a 60 mesh screen for a maximum fiber size of 60 mesh. IGC columns were packed with the fibers and the samples were conditioned at 103°C in the IGC with 15 standard

TABLE II  
Dispersive Energy as a Function of Temperature and Regressed Value at 20°C for Various Fiber Types Calculated by the Schultz and Lavielle Method

Fiber type	Dispersive energy (mJ/m <sup>2</sup> )				Coefficient of determination
	40 (°C)	35 (°C)	30 (°C)	20 (°C)	
Grass fibers					
Wheat straw	35.4	37.5	38.0	40.9	0.90
Wheat pulp bleached	38.5	39.4	40.6	42.6	0.99
Rice hulls	39.4	40.2	41.9	44.2	0.96
Reed	37.2	38.3	39.6	41.9	1.00
Bast fibers					
Hemp	35.9	37.8	39.5	43.1	1.00
Flax	34.9	37.0	38.7	42.7	1.00
Kenaf	36.9	38.3	40.0	43.1	1.00
Jute	43.5	42.5	41.9	40.2	0.98
Leaf fibers					
Abaca	36.2	36.2	36.0	35.8	0.90
Sisal	41.2	39.8	38.4	35.5	1.00
Seed hair fibers					
Cotton	38.7	38.3	39.5	40.0	0.45
Poplar seed	38.9	38.7	39.9	40.6	0.66
Fruit hair fibers					
Kapok	37.7	37.9	39.5	41.1	0.85
Coir	36.4	37.7	39.1	41.8	1.00

TABLE III  
Medians of Measured Dispersive Energies at 40°C and Collected Cellulose, Lignin, and Hemicellulose Contents from Literature Sources for the Five Natural Fiber Subgroups

Fiber group	Dispersive energy mJ/m <sup>2</sup> at 40°C	Cellulose %	Lignin %	Hemicellulose %
Grass fibers	37.63	32.00	14.00	25.50
Bast fibers	37.80	64.50	11.50	18.50
Leaf fibers	38.70	59.80	9.75	17.03
Seed fibers	38.80	87.00	0.95	4.00
Fruit fibers	37.05	24.20	29.75	25.83

cubic centimeters, (sccm), of helium until the flame ionizing detector recorded a background signal of <5 pA at 30°C.

### IGC measurements

After conditioning the fibers, experiments were conducted using a fully automated Surface Measurements Systems SMS IGC with head space temperature control. Custom silane treated glass tubes are used for the SMS IGC at the temperature of 30°C, 35°C, and 40°C and a flow rate of 10 sccm. Vapors of HPLC grade polar and nonpolar probes were sampled with microsyringe and an infinitely dilute concentration of probe was injected into the packed column and the retention time measured by a flame ionization detector. An infinitely dilute sample of methane was injected to determine the dead time in the column. The probe retention time and the methane retention time were entered into eq. (1) with the mass of the packed material in the column and were used for calculating the dispersive energy and  $K_a$ ,  $K_b$  of the fibers. Calculations were done using an Excel spreadsheet and packaged software from SMS. To calculate  $K_a$  and  $K_b$  eq. (12) is written in  $y = mx + b$  form and AN\* used where AN\* is in energy/mol because AN is a unitless value:

$$\frac{-\Delta H_A^{AB}}{4.184 \text{ AN}^*} = \frac{\text{DN}}{\text{AN}^*} K_a + K_b \quad (13)$$

values of DN and AN\* were taken from the literature and are reported in Table I for the probes used in IGC.

## RESULTS AND DISCUSSION

The dispersive energies, molecular compositions, acid–base characteristics, surface topography, and visual scans of the various fiber surfaces are presented.

### Dispersive energies

Results for the dispersive component of the surface energy,  $\gamma_S^d$ , ranged from 35.5 mJ/m<sup>2</sup> for sisal to 44.2 mJ/m<sup>2</sup> for rice hulls at 20°C. The dispersive surface energy for all fiber types are shown in Table II.

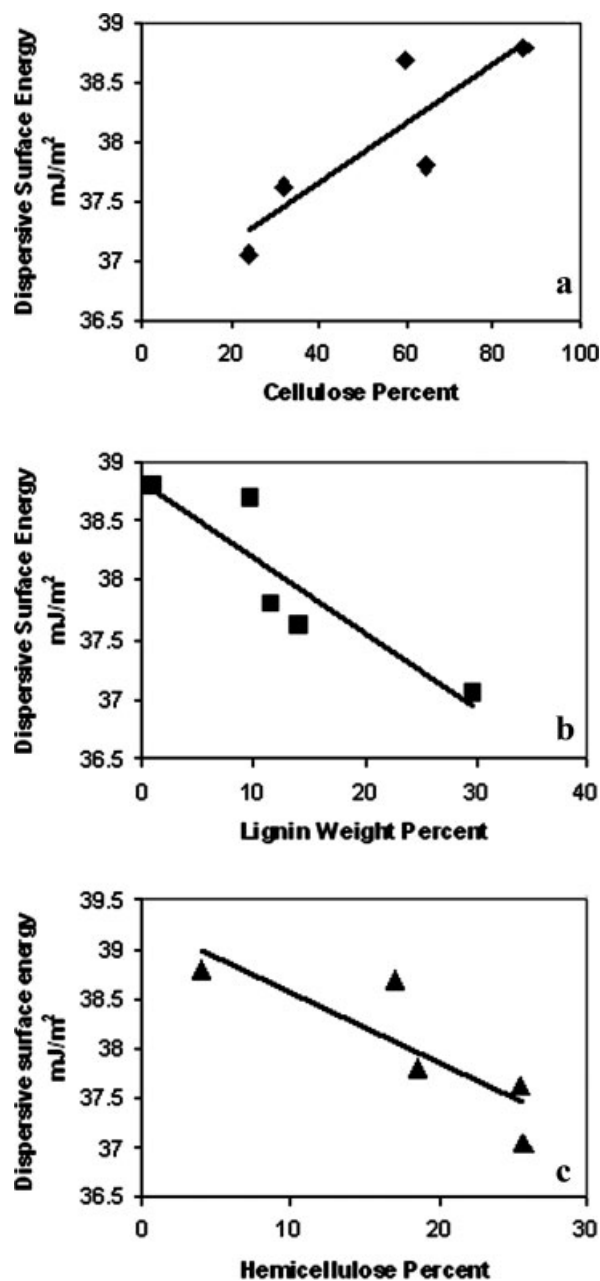
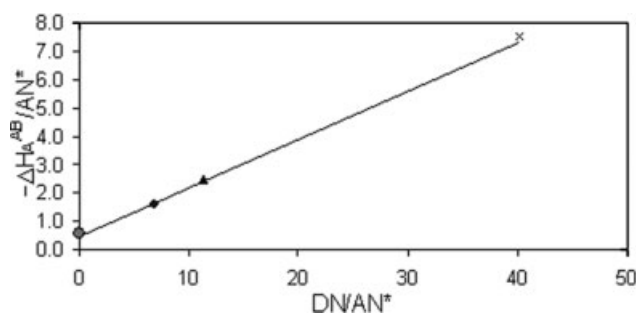


Figure 1 Dispersive surface energy as a function of (a) percent cellulose, (b) percent lignin, and (c) percent hemicellulose composition and dispersive surface energy values from Table III.



**Figure 2** Relationship for determining  $K_a$  and  $K_b$  using data from the polarization method at 30°C, 35°C, and 40°C for the flax fiber with chloroform ●, ethyl acetate ▲, acetone ◆, and tetrahydrofuran x.

Explanations for differences in the surface energies may be determined by looking at the chemical composition of the fibers. With the exception of poplar seed hairs and the wheat pulp fibers an extensive data collection was acquired from literature for all fiber types featuring cellulose, hemicellulose, and lignin percentages.

### Statistical analysis

Nonparametric medians were calculated for each fiber group (Table III) and these values were rank-

**TABLE IV**  
 $K_a$  and  $K_b$  for All 14 Fiber Types

Fiber type	$K_a$	$K_b$	Coefficient of determination
Flax	0.17	0.49	1.00
kenaf	0.07	0.32	0.95
kapok	0.14	1.05	0.97
cotton	0.06	0.50	0.98
hemp	0.16	0.49	0.99
Rice	0.21	0.38	1.00
Poplar seed hair fibers	0.10	0.42	1.00
Wheat pulp bleached	0.10	0.47	0.92
Wheat straw	0.15	0.70	1.00
Reed	0.15	0.61	1.00
Coir	0.19	0.20	1.00
Sisal	0.38	0.74	1.00
Abaca	0.12	0.59	0.99
Jute	0.01	0.00	0.98

correlated with each other by Spearman's rank correlation coefficient.

Significant rank correlations were found between cellulose ( $r = 0.9$ ,  $P < 0.05$ ), lignin ( $r = -1.0$ ), and hemicellulose ( $r = -1.0$ ), respectively, and dispersive energy measured at 40°C. Dispersive energies at the other temperatures did not show significant rank correlations. The data found to correlate by Spearman's analysis are presented in Figure 1.

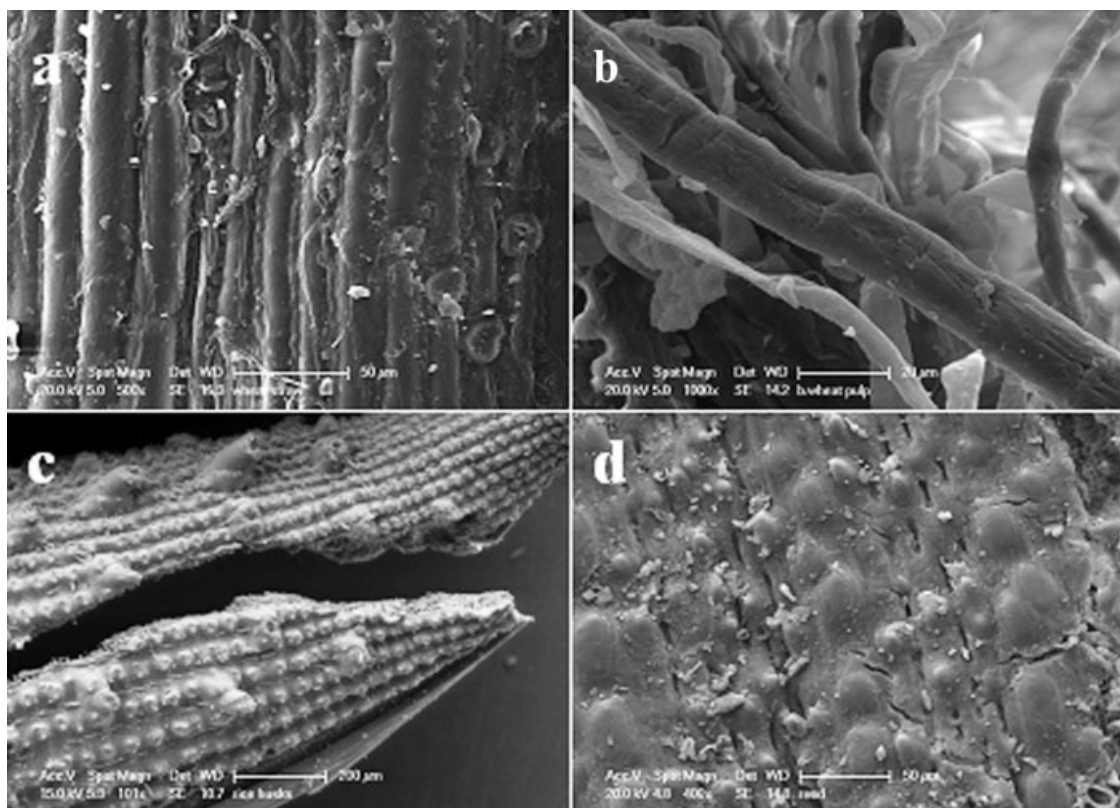


**Figure 3** SEM images of the measured grass fibers. (a) wheat straw fibers, (b) bleached wheat pulp fibers, (c) rice hulls, and (d) reed grass.

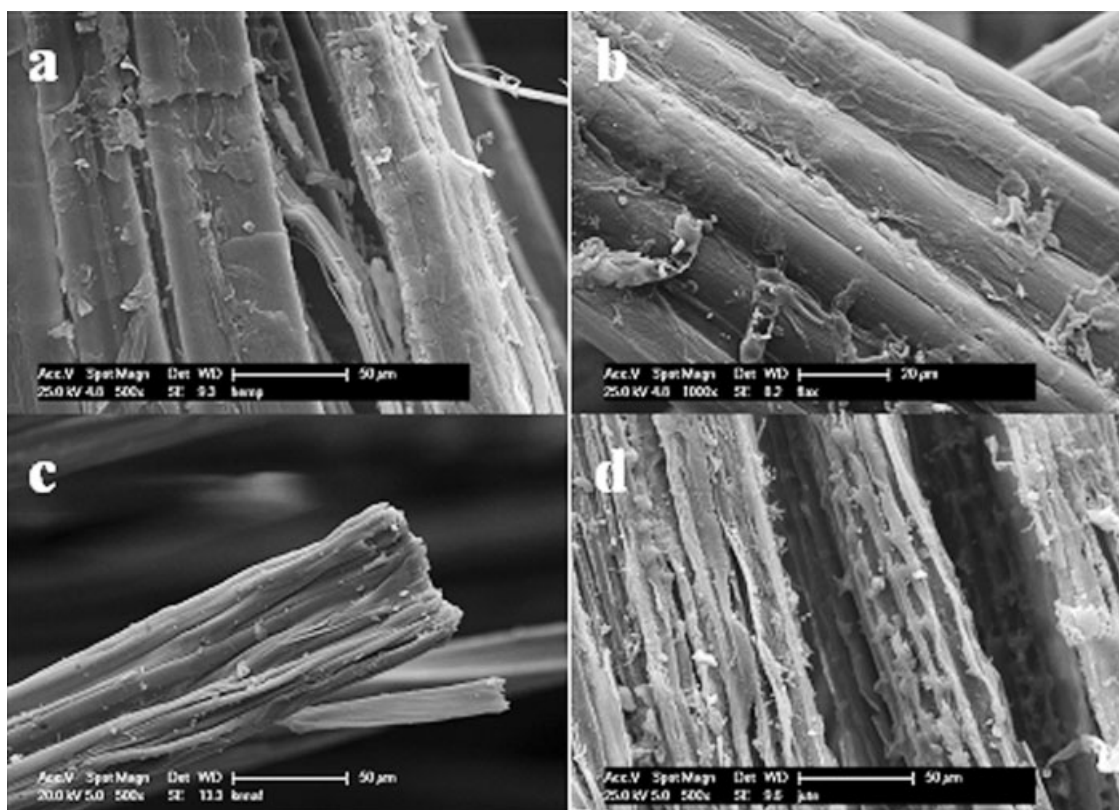


**Figure 4** SEM image of the measured bast fibers. (a) hemp, (b) flax, (c) kenaf, and (d) jute.

In Figure 1(a), the surface energy increases as a function of cellulose as a component in the composition of the fibers,  $R^2 = 0.73$ . This is consistent with results found by Parades et al.,<sup>19</sup> where hemicellulose extract was removed from red maple and the crystallinity and surface energy increased with increased cellulose surface content. Mills et al.<sup>20</sup> reported results for IGC with a hemicellulose extract from red maple comprised of approximately 70 weight percent hemicellulose and 15 weight percent lignin of  $34.7 \text{ mJ/m}^2$  at  $40^\circ\text{C}$  consistent with both part B,  $R^2 = 0.80$ , and C,  $R^2 = 0.70$ , of Figure 1

where as the content of lignin and hemicellulose increases the dispersive surface energy decreases.

Although there was a clear association between the fiber chemistry and the measured dispersive energy levels, we also hypothesize that only certain functional groups contribute to the surface energy of the fibers. The energy of the surface is dependent on how long since the material has been through surface conditioning processes. A freshly sanded or mechanically conditioned surface should have the highest surface energy and the energy decreases over time since last surface conditioning event due to low-molecular

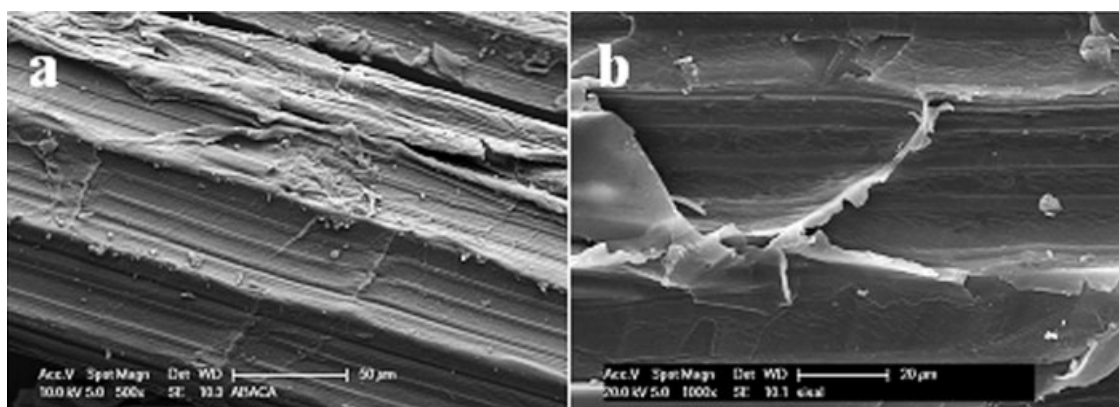


**Figure 5** SEM image of the measured leaf fibers. (a) abaca and (b) sisal.

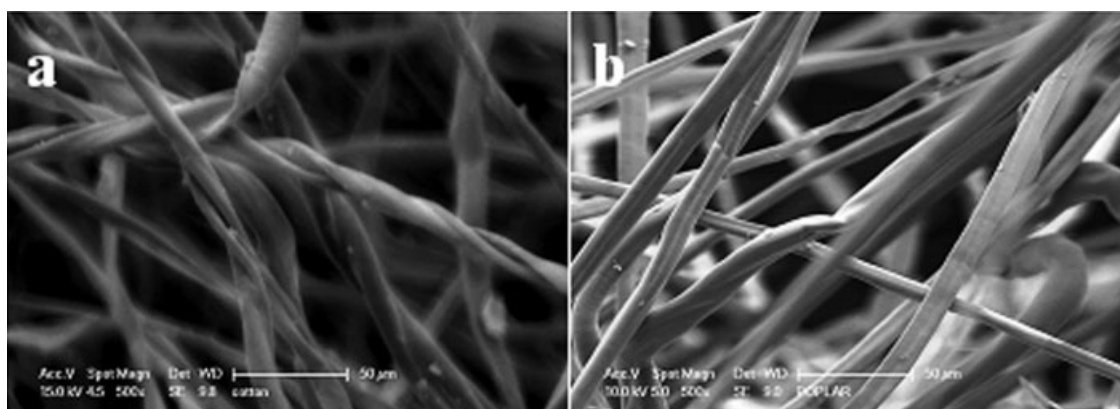


**Figure 6** SEM image of the seed hair fibers. (a) cotton and (b) poplar.

weight extractives migrating to the surface inactivating the surface<sup>21</sup> or deactivating by thermal drying.<sup>22</sup> Although significant, the dispersive energy differences among fibers are not considered to be of high practical impact. Further, fibers were sheared in a Wiley mill passing through a [1/2] mm screen until a 60 mesh particle size was achieved and then packed and weighed in the IGC column and conditioned. Therefore, the highest energy values for the materials should be achieved if the material is processed, conditioned, and tested within a 3 day period. Also, as IGC is a method using infinitely dilute gas phase probes, it is generally accepted that probes preferentially select the highest energy sites of a heterogeneous surface as the low concentration of probe molecule selects the highest energy sites on the material first for bonding, this might give more weight to the argument that the surface energy calculated is the highest to be expected. More expressed surface energies would be found for the various fiber types had no surface modifications occurred, either mechanical or chemical, which would have been more indicative for the varying molecular compositions.

These surface energy values were compared with results in the literature. Gulati and Sain,<sup>23</sup> reported a dispersive energy for hemp at 40°C being 38 mJ/m<sup>2</sup>

(35.9 mJ/m<sup>2</sup>) Reutenauer and Thielmann<sup>24</sup> report a dispersive energy for cotton of 35.18 mJ/m<sup>2</sup> (39.5 mJ/m<sup>2</sup>) at 30°C; and Tshabalala reports a value of 40 mJ/m<sup>2</sup> (36.9 mJ/m<sup>2</sup>) at 40°C for Kenaf.<sup>25</sup> The reported Kenaf and Hemp values are slightly higher than found in this study and the cotton values are lower.

#### Donor acceptor analysis

Graphs were made and regressed for each of the 14 fiber types as is shown in Figure 2 using flax fiber as an example. Table IV contains all the  $K_a$  and  $K_b$  values determined from the regressions with the coefficient of determination presented. Because of space constraints, all 14 graphs are not shown and the coefficient of determination should be sufficient to evaluate linearity. From the regression and eq. (13), the values of  $K_a$  and  $K_b$  for the fibers were determined.

#### Surface scans and molecular compositions

SEM images were made from all investigated fiber types (Figs. 3–7).

The grass-fiber group has a strongly structured surface with thick epicuticular wax layers. These wax-cuticle layers are rather thick and might experience

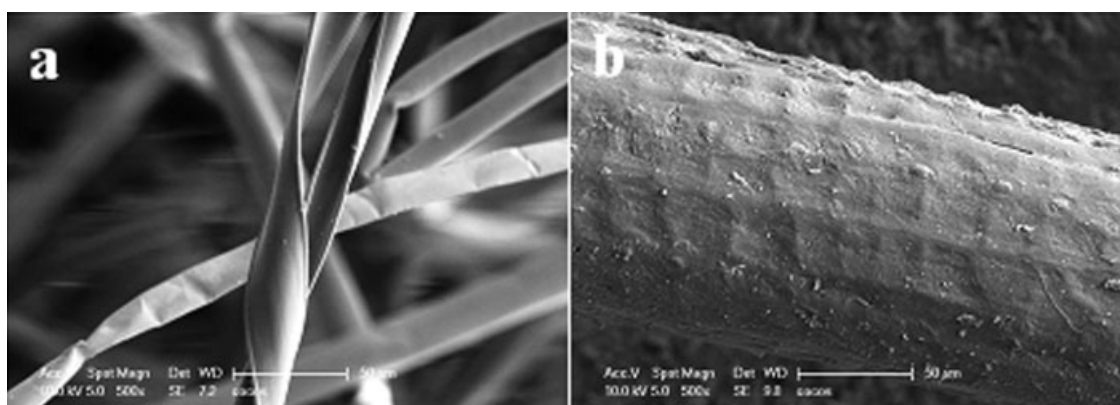


**Figure 7** SEM image of the measured fruit hair fibers. (a) kapok and (b) coir.

some mechanical removal during processing.<sup>26</sup> Individual wheat fibers are seen with the pulped version [Fig. 3(b)] and surfaces are much smoother.

Bast-fiber surfaces are generally smoother with epicuticular wax layers mostly removed during the retting process.<sup>27</sup> The leaf-fibers abaca and sisal have very similar rippled surfaces with visible epicuticular wax and fat layers.

With the exception of coir, the two fruit-fiber types exhibit thin fibers with poplar seed hairs being the thinnest (under 10  $\mu\text{m}$ ). Surfaces are much smoother than the other natural fiber types and the extent of epicuticular wax layers is limited. Coir fiber surfaces are much thicker (>100  $\mu\text{m}$ ) but also smooth with a slight rippled structure that include pit formations.<sup>27</sup>

In general, most of the fibers displayed similar  $K_a$ 's and  $K_b$ 's; however, looking at kapok and cotton, as examples, kapok has both a higher  $K_a$  and  $K_b$ , this result could be related to kapok only containing 13% cellulose and cotton having 92% cellulose. Perhaps, extractives on the surface or the aromatic nature of lignin may be contributing to the large electron donor nature of the kapok versus the cotton. Jute displayed rather a nonreactive surface. This may be due in part to no pretreatment other than mechanical shearing in a Wiley mill but leads to interesting questions about the surface of the fibers. Many fiber types are covered with waxy coatings that may deactivate the surface. In Figure 8(a–c), it is apparent that there is a wide range in lignin and cellulose composition; however, the hemicellulose concentration stays relatively constant. The only large changes in the acid–base characteristics are seen in the extreme cases of cotton and kapok. This indicates that there may be a sizable amount of surface area of the fiber comprising hemicellulose as this component changes the least amount from fiber to fiber. Also, Figures 3–7 show the topography of the fibers and it's apparent that the surfaces are very different on a micrometer scale and although this should not impact interactions on a molecular scale, the interactions between a matrix material and the fibers may be significantly impacted by the surface geometries. More analytical work needs to be done to determine the exact nature of the fiber surfaces to correlate with this work.

### Suggestions for composite fabrication

- Most of the fiber types have a waxy layer that may act as a weak boundary layer in the cohesion and adhesion interactions in a composite and as such should be either mechanically or chemically removed before use in a composite material.
- Hemicellulose and lignin tend to lower the surface energy of fiber surfaces and some chemical

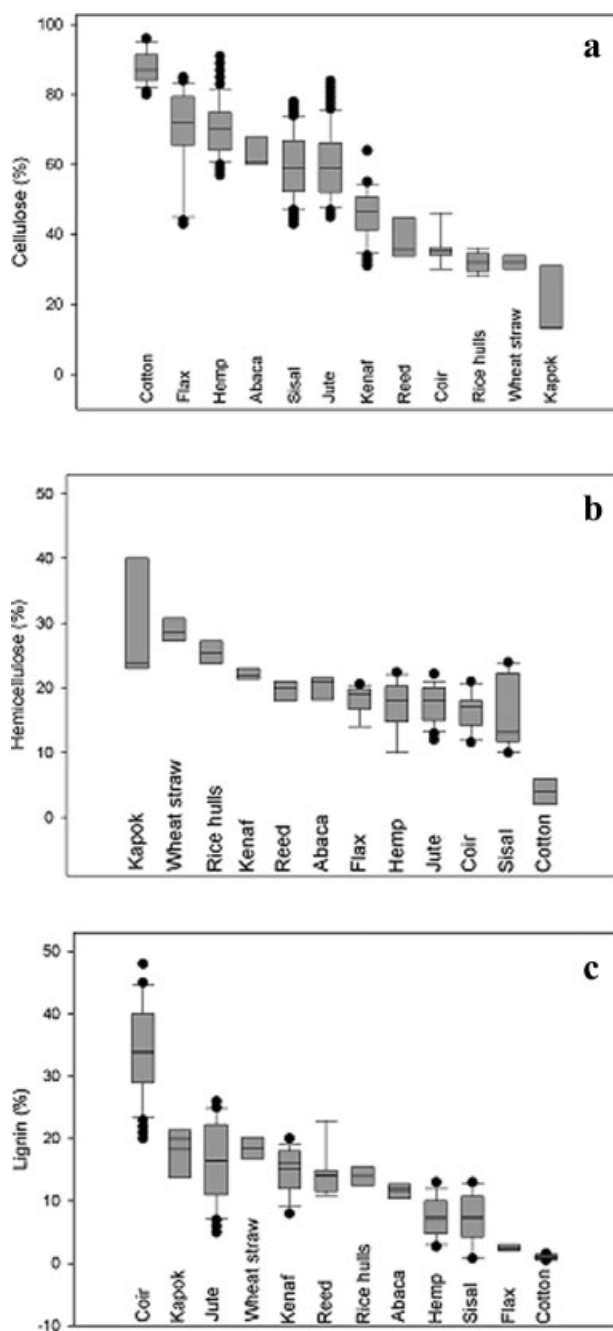


**Figure 8** Literature values for composition of fibers. (a) cellulose, (b) hemicellulose, and (c) lignin.<sup>18,28–52,55</sup>

treatments to lower there surface concentrations may be needed.

- Mechanical treatments of the surface of fibers may create significant increases in surface area that may lead to better bonding and cohesion in a composite material.

### CONCLUSIONS

Fourteen different fiber types were tested using IGC. From these data, dispersive surface energies were



calculated and compared and found to be between 35.5 mJ/m<sup>2</sup> and 44.2 mJ/m<sup>2</sup> for all the fiber types at 20°C. There is a clear association between the fiber composition and the measured dispersive energy levels at 40°C as was found by Spearman's rank correlation coefficient and is displayed in Figure 1(a–c). The only large changes in the acid base characteristics are seen in the extreme cases of cotton and kapok. This indicates that there may be a sizable amount of surface area of the fiber comprising hemicellulose as this component changes the least amount from fiber to fiber. The SEM micrographs show that the grass-fiber group has a strongly structured surface with thick epicuticular wax layers on the surface. Bast-fiber surfaces are generally smoother than the other fiber types. Fruit-fiber types exhibit thin fibers. The leaf-fibers abaca and sisal have very similar rippled surfaces with visible epicuticular wax and fat layers.

## References

- Matuana, L. M.; Park, C. B.; Balatinecz, J. J. *Polym Eng Sci* 1998, 38, 765.
- Woodhams, R. T.; Thomas, G. *Polym Eng Sci* 1984, 24, 1166.
- Kazayawoko, M.; Balatinecz, J. J.; Matuana, L. M. *J Mater Sci* 1999, 34, 6189.
- Matuana, L. M.; Woodhams, R. T.; Balatinecz, J. J.; Park, C. B. *Polym Compos* 1998, 19, 446.
- Tze, W. T. Y.; Wälinder, M. E. P.; Gardner, D. J. *J Adhesion Sci Technol* 2006, 20, 743.
- Clemons, C. M.; Giacomini, A. J.; Koutsky, J. A. *Polym Eng Sci* 1997, 37, 1012.
- Lundqvist, Å.; Ödberg, L. *Fundamentals Papermaking Mater* 1997, 2, 751.
- Jacob, P. N.; Berg, J. C. *Langmuir* 1994, 10, 3086.
- Carvalho, M. G.; Santos, J. M. R. C. A.; Martins, A. A.; Figueiredo, M. M. *Cellulose* 2005, 12, 371.
- Boras, L.; Sjostrom, J. *International Symposium on Wood and Pulping Chemistry, Proceedings, ISWPC; v 2* 1997; p 9–1.
- Chtourou, H.; Riedl, B.; Kokta, B. V. *J Adhesion Sci Tech* 1995, 9, 551.
- Dorris, G. M.; Gray, D. G. *J Colloid Interface Sci* 1980, 77, 353.
- Riedl, B.; Matuana, L. M. *Encycl Surface Colloid Sci* 2002, 2842.
- Schultz, J.; Lavielle, L. *ACS Symp Ser*, 1989, 391, 185.
- Schultz, J.; Lavielle, L. *Langmuir* 1991, 7, 978.
- Donnet, J. B.; Park, S. J.; Balard, H.; *Chromatographia* 1991, 31(9/10), 434.
- Gutmann, V. *The Donor Acceptor Approach to Molecular Interactions*; Plenum: New York, 1978; Chapter 2.
- Franck, R. R. In: *Bast and Other Plant Fibres*; Franck, R. R., Ed.; CRC: Boca Raton, 2005; p 1.
- Parades, J.; Mills, R.; Gardner, D.; Shaler, S.; *Wood Fiber Sci*, submitted.
- Mills, R.; Jara, R.; Gardner, D.; van Heiningen, A. *J Wood Chem and Tech*, submitted.
- Back, E. L. *Forest Prod J* 1991, 41, 30.
- Christiansen, A. W. *Wood Fiber Sci* 1990, 22, 441.
- Gulati, D.; Sain, M. *Polym Eng Sci* 2006, 46, 269.
- Reutenauer, S.; Thielmann, F. *J Mater Sci* 2003, 38, 2205.
- Tshabalala, M. A. *J Appl Polym Sci* 1997, 65, 1013.
- Ouajai, S.; Shanks, R. A. *Polym Degrad Stabil* 2005, 89, 327.
- Bismarck, A.; Mohanty, A. K.; Aranberri-Askargorta, I.; Czaplá, S.; Misra, M.; Hinrichsen, G.; Springer, J. *Green Chem* 2001, 3, 100.
- Ass, B. A. P.; Ciacco, G. T.; Frollini, E. *Bioresour Technol* 2006, 97, 1696.
- Mazumdera, B. B.; Nakgawa-Izumi, A. B.; Kuroda, K.; Ohtani, A. Y.; Sameshima, K. *Ind Crops Products* 2005, 21, 17.
- Bismarck, A.; Mohanty, A. K.; Aranberri-Askargorta, I.; Czaplá, S.; Misra, M.; Hinrichsen, G.; Springer, J. *Green Chem* 2001, 3, 100.
- Clemons, C. M.; Caulfield, D. F. *Natural Fibers*. In Chapter 11 of *Functional Fillers for Thermoplastics*; Xanthos, M., Ed.; Wiley-VCH Verlag GmbH & Co. KGaA, 2005; p 195.
- Dien, B. S.; Jung, H. G.; Vogel, K. P.; Casler, M. D.; Lamb, J. F. S.; Weimer, P. J.; Iten, L.; Mitchell, R. B.; Sarath, G. *Biomass Bioenergy* 30: 880–891.
- Han, J. S. In: *Proceedings of the Korean Society of Wood Science and Technology Annual Meeting*, Seoul, Korea; The Korean Society of Wood Science and Technology, 1998; p 3.
- Hori, K.; Flavier, M. E.; Kuga, S. *J Wood Sci* 2000, 46, 401.
- Hurter, A. M. *Proceedings of TAPPI Pulping Conference*, New Orleans, LA, USA; Book; TAPPI Press: Atlanta, Georgia, 1988; 1, p 139.
- Jose, C.; del Rio, G. A. *J Agric Food Chem* 2006, 54, 4600.
- Lam, T. B. T.; Hori, K.; Iiyama, K. *J Wood Sci* 2003, 49, 255.
- Mwaikambo, L. Y. *African J Sci Technol* 2006, 7, 120.
- Mwaikambo, L. Y.; Ansell, M. P. *J Mater Sci Lett* 2001, 20, 2095.
- Nilsson, T. *Studia Forestalia Suecica* 1974, 117, 1.
- Rahman, M. M.; Khan, M. A. *Compos Sci Technol* 2007, 67, 2369.
- Reddy, N.; Yang, Y. *Trends Biotechnol* 2005, 23, 22.
- Reddy, N.; Salam, A.; Yang, Y. *Macromol Mater Eng* 2007, 292, 458.
- Rowell, R. M. *A New Generation of Composite Materials from Agro-Based Fiber*. In *Proceedings of 3rd International Conference on Frontiers of Polymers and Advanced Materials*, Kuala Lumpur, Malaysia; Plenum Press: New York, 1995.
- Rowell, R. M. In: *Research in Industria Application of Non Food Corps. I. Plant Fibres*; Oleson, O., Rexen, F., Larsen, J., Eds.; *Proceedings of a Seminar*, May 1995; Academy of Technical Science: Copenhagen, 1995; p 27.
- Rowell, R. M.; Han, J. S.; Rowell, J. S. In: *Natural Polymers and Agrofibers Composites*; Frollini, E., Leão, A. L., Mattoso, L. H. C., Eds.; USP-IQSC: São Carlos - Brazil - São Carlos/UNESP: Embrapa Instrumentação Agropecuária/Botucatu, 2000; p 115.
- Silva, G. G.; De Souza, D. A.; Machado, J. C.; Hourston, D. J. *J Appl Polym Sci* 2000, 76, 1197.
- Sun, R. C.; Fang, J. M.; Goodwin, A.; Lawther, J. M.; Bolton, A. *J Carbohydr Polym* 1998, 37, 351.
- Thygesen, A.; Oddershede, J.; Lilholt, H.; Thomsen, A. B.; Stahl, K. *Cellulose* 12, 563.
- Thygesen, A.; Daniel, G.; Lilholt, H.; Thomsen, A. B. *J Natural Fibers* 2006, 2, 19.
- van Dam, J. E. G.; van den Oever, M. J. A.; Keijsers, E. R. P.; van der Putten, J. C.; Anayron, C.; Josol, F.; Peralta, A.; *Ind Crops Products* 2006, 24, 96.
- Ververis, C.; Georghiou, K.; Christodoulakis, N.; Santas, P.; Santas, R. *Ind Crop Product* 2004, 19, 245.
- Jeffree, C. E.; Baker, E. A.; Holloway, P. J. *New Phytol* 1975, 75, 539.
- Park, S. J.; Donnet, J. B. *J Colloid Interface Sci* 1998, 206, 29.
- Mwaikambo, L. Y.; Ansell, M. P. *J Appl Polym Sci* 2002, 84, 2222.